Sensors and Materials, Vol. 27, No. 1 (2015) 1–10
MYU Tokyo

S & M 1040

Vibration Analysis and Evaluation of Piezoelectric Micromachined Ultrasonic Transducers Using Epitaxial Pb(Zr, Ti)O_3 Thin Film

Daisuke Takashima, Katsuya Ozaki, Masato Nishimura, Nagaya Okada[1], Daisuke Akai[2,*] and Makoto Ishida

Dept. of EeiE, Toyohashi University of Technology,
1-1 Hibarigaoka, Tenpaku, Toyohashi, Aichi 441-8580, Japan
[1]Honda Electronics Co., Ltd., 20 Oyamazuka, Oiwa, Toyohashi, Aichi 441-3193, Japan
[2]Electronics-Inspired Interdisciplinary Research Institute, Toyohashi University of Technology,
1-1 Hibarigaoka, Tenpaku, Toyohashi, Aichi 441-8580, Japan

(Received July 13, 2014; accepted November 20, 2014)

Key words: pMUT, ultrasonic, PZT, γ-Al_2O_3, FEM

To improve the transmitting and receiving characteristics of piezoelectric micromachined ultrasonic transducers (pMUTs), the thickness of the diaphragm material SiN_x of the pMUT was investigated by vibration analysis using the finite element method (FEM). The vibration magnitudes increase 1.7-fold by changing the SiN_x thickness from 1.0 to 0.5 μm as determined by the FEM results. A pMUT with a new structure that has a 0.5-μm-thick SiN_x layer was fabricated and evaluated. The vibration of the pMUT was evaluated by a laser Doppler vibrometer (LDV), and the vibration magnitude of the fabricated pMUT was threefold that of our previously reported pMUT. Ultrasonic characteristics such as transmitted ultrasonic sound pressure and ultrasonic sensitivity are also evaluated and compared with those of the previous pMUT. The fabricated pMUT shows 11 times larger transmitted ultrasonic sound pressure and 5 times larger ultrasonic sensitivity than those exhibited by the previous pMUT.

1. Introduction

Ultrasonic technologies are widely used for non-destructive evaluations, especially in medical diagnostics systems.[1–4] Ultrasonic transducers used in medical applications require integration of endoscopy with micro-scale two-dimensional (2D) ultrasonic transducer arrays for high-resolution three-dimensional (3D) imaging. To fulfill this requirement, micromachined ultrasonic transducers (MUTs) on Si substrates have been studied by many groups. MUTs are much smaller than conventional ceramic transducers and they are classified into two types. A capacitive MUT (cMUT) uses electrostatic-driven surface micromachined membranes on Si substrates, and cMUTs

*Corresponding author: e-mail: akai@vbl.tut.ac.jp

have been widely studied because of their ease of manufacturing by the batch process and possibility of integrating signal processing circuitry.[5,6] The other is a piezoelectric MUT (pMUT), which is driven by piezoelectric materials such as lead zirconate titanate (PZT) film.[2–4] pMUTs have a lower operating voltage, higher transmission power, and higher sensitivity than cMUTs. However, pMUTs using good quality piezoelectric thin films are difficult to integrate with Si-LSI because it is impossible to fabricate epitaxial piezoelectric thin films on a common insulating layer of SiO_2.

We have proposed and fabricated pMUT arrays using epitaxial PZT thin films on epitaxial γ-Al_2O_3/Si substrates to integrate with Si-LSI and improve the sensitivity compared with those of polycrystalline PZT films, and have reported the pMUT's characteristics, such as transmitted sound pressure and sensitivity.[7–9] However, we could not obtain 3D images by using the pMUT because their evaluated characteristics are not sufficient to transmit and receive ultrasonic waves by the same pMUT. Therefore, it is necessary to increase the transmitting power and the sensitivity of the pMUT.

Figure 1 shows the structure of our proposed circular pMUT using epitaxial γ-Al_2O_3 film as an insulating layer on a Si substrate. It consists of a PZT thin film sandwiched between a top electrode $SrRuO_3$ (SRO) and a bottom electrode SRO/Pt, a diaphragm material SiN_x, and a wiring material Al-Si. The SiN_x layer also plays the role of an insulating layer between the Al-Si wiring and the SRO/Pt bottom electrode. The surface of the pMUT is covered with a photoresist to protection against water. The diameter of the pMUT is 100 μm in consideration of the operating frequency for typical medical applications of 1–5 MHz.[9] The pMUT is a multilayer structure fabricated of the PZT, electrodes, SiN_x, and photoresist, hence its characteristics are affected not only by the piezoelectric property of PZT but also by other structural properties, such as its hardness, weight, diameter, and thickness. In particular, the thickness of the diaphragm material SiN_x greatly affects on the characteristics of the pMUT because SiN_x is the hardest material among the structural materials of the pMUT (material properties are described in § 2.1) however, it is easy to control the thickness. The SiN_x layer thickness of the pMUT in our previous work (ref. 9) is 1.0 μm, which is not an optimal value. Therefore, we expect to obtain better characteristics by optimizing it.

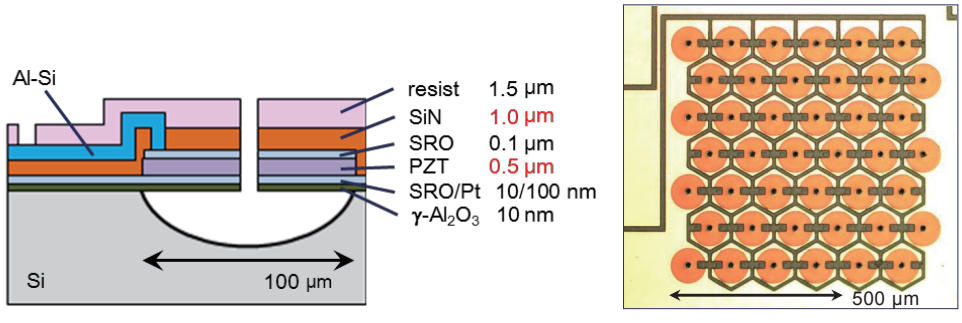

(a) (b)

Fig. 1. (Color online) (a) Schematic cross section and (b) image of our proposed pMUT.

In this study, to improve the characteristics of the pMUT, the thickness of the diaphragm material SiN_x was investigated on the basis of vibration analysis by the finite element method (FEM). As a result of the FEM analysis, an improved pMUT was fabricated and evaluated. Characteristics of the pMUT, such as vibration magnitude, transmitting ultrasonic power, and ultrasonic sensitivity, are compared with those of the pMUT we previously reported.

2. Experimental Procedure

2.1 *Vibration analysis*

ANSYS was used for FEM analysis, and Fig. 2 shows the analysis model, which consists of a 100-μm-clamped circular diaphragm part. In the analysis model, the 10-nm-thick γ-Al_2O_3 layer and SRO bottom electrode layer are neglected to simplify the model. These layers are too thin to affect the simulation results. Table 1 shows the material parameters, such as Young's modulus, Poisson's ratio, and density, of each layers used in the analysis model.[10–13] In addition, the PZT layer requires piezoelectric constant parameters, which are shown in Table 2.[14] In the model, a polyimide layer is used instead of the photoresist layer because the polyimide and the photoresist are both polymer materials and have a similar Young's modulus, Poisson's ratio, and density.

To investigate the vibration of the pMUT, two types of analyses were conducted: modal analysis and frequency analysis. PMUTs operate as resonant devices, because the sensitivity and transmitting power of the pMUT at the resonance frequency are much larger than those at other frequencies. Modal analysis is effective to analyze a structure's resonance frequencies and resonant mode shapes determined by many perspectives, such as the shape, boundary condition, Young's modulus, and density. Frequency analysis was used to analyze the vibration magnitude of the pMUT by applying a 4 V_{pp} sine wave at the resonance frequency. An improved pMUT structure was fabricated and evaluated by FEM analysis.

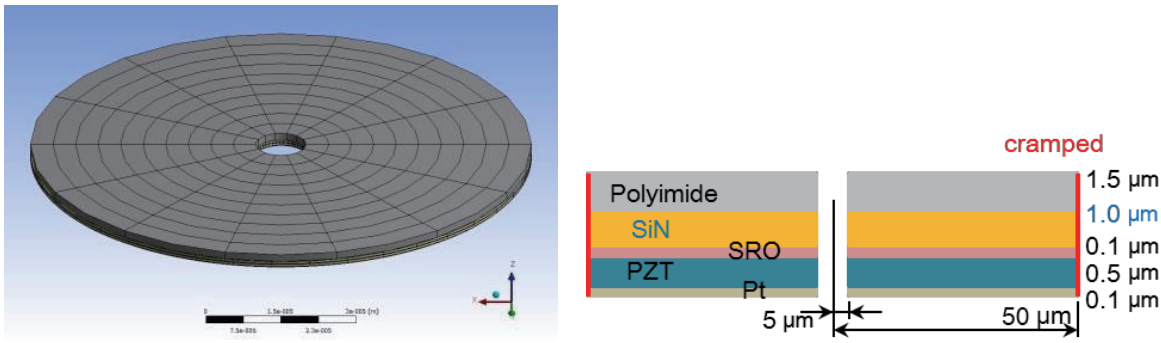

(a) (b)

Fig. 2. (Color online) (a) Analysis model of diaphragm of pMUT for FEM and (b) materials and sizes of model.

Table 1
Material properties for FEM analysis (1).

Material	Density (kg/m^3)	Young's modulus (GPa)	Poisson's ratio (−)
Pt[10]	21500	171	0.39
SRO[11]	6500	190	0.3
SiN[12]	3100	285	0.2
Polyimide[13]	1420	2.6	0.34

Table 2
Material properties for FEM analysis (2).

Material	Elastic modules ($\times 10^{11}$ N/m^2)	Piezoelectric constant (C/m^2)	Dielectric constant (−)	Density (kg/m^3)	tanδ
PZT[14]	$c_{11} = c_{22} = 1.32$, $c_{12} = 0.71$, $c_{13} = c_{23} = 0.73$, $c_{33} = 1.15$, $c_{44} = 0.3$, $c_{55} = c_{66} = 0.26$	$e_{33} = 14.1$, $e_{31} = -13.1$, $e_{15} = 10.5$	854	7700	0.03

2.2 *Fabrication*

The pMUT, which has a 100-μm-diameter circular diaphragm, was fabricated by the following process. First, the epitaxial γ-Al_2O_3 thin film was grown on a 4-inch Si(111) substrate by molecular beam epitaxy.[15] Then, a (111)-oriented SRO/Pt stacked bottom electrode was deposited by RF-magnetron sputtering on the γ-Al_2O_3 layer. Piezoelectric PZT (Zr/Ti ratio of 52/48) thin films were deposited by a conventional sol-gel method, and crystallized at 650 °C for 90 s by rapid thermal annealing (RTA) in oxygen atmosphere. A SRO top electrode layer was sputtered on the PZT layer, and the top SRO layer, PZT layer, and bottom SRO/Pt layer were patterned by conventional lithography technique and inductivity coupled plasma reactive ion etching. A SiN_x film was formed by plasma-enhanced chemical vapor deposition as an insulating layer between the Al-Si wiring and bottom Pt electrode. To encapsulate the Al-Si wiring and to form the diaphragm, a photoresist layer was then applied, except at the etching holes, for the formation of diaphragm and bonding pads. Following resist coating, the wafer was diced into 5 × 5 mm^2 chips by a stealth laser dicing system. Then, Si below the diaphragm area was etched by XeF_2 gas from the top side of the chips. A spherical cavity of 100 μm diameter was formed below the insulator/PZT/metal stacked structure after this etching process.

After XeF_2 etching, chips were glued onto the printed circuit board and wirebonded to the package, as shown in Fig. 3. Bonding wires were covered with epoxy to enable immersion in water during measurement.

2.3 *Evaluation*

The mechanical resonances and vibration magnitudes of the pMUT were characterized and visualized using a scanning laser Doppler vibrometer (LDV) (MSA-500, Polytec)

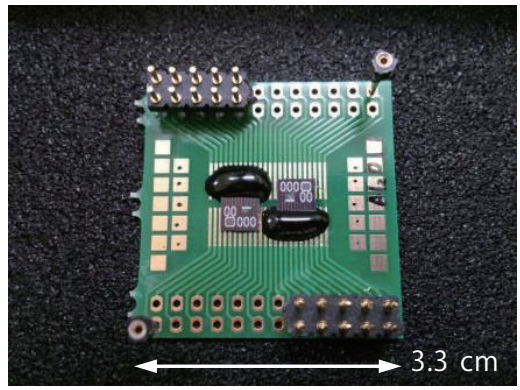

Fig. 3. (Color online) Photograph of pMUT chips packaged on printed circuit board.

in air. Ultrasonic characteristics were measured using an acoustic intensity measurement system (AIMS).[16] Figure 4(a) is a schematic of the ultrasonic transmitting measurement system. A function generator was used for applying voltage to the pMUT, and the generated ultrasonic waves were received by a hydrophone placed about 1.0 cm opposite the pMUT. Using the hydrophone, it is possible to evaluate the sound pressure of ultrasonic waves underwater. The received signals were observed using a digital oscilloscope (DSO1022A, Agilent) through an amplifier (40 dB). An ultrasonic receiving experimental system is shown in Fig. 4(b). Ultrasonic waves generated by a conventional ceramic ultrasonic transducer were received by the pMUT, and the output signals of the pMUT were measured by the oscilloscope through the 40-dB amplifier. Ultrasonic sensitivities of the pMUT were calculated from the generated ultrasonic sound pressure and the output signal.

3. Results and Discussion

3.1 *FEM results*

Figure 5 shows the analysis results of resonant mode shapes and resonance frequencies from the 1st to 4th mode resonance of the pMUT. The pMUT has many resonant mode shapes, and the 1st resonant mode is expected to radiate ultrasonics very effectively into the surrounding medium. The other resonant modes could not radiate sound effectively, because one region of the diaphragm pushes the medium up while the other region pulls the medium down. Therefore, only the vibration magnitude of the 1st resonant mode was investigated in this study. A 4 V_{pp} sine wave, which has 1st resonance frequency, was applied between the top electrode and the bottom electrode of the pMUT. Vibration magnitudes of the pMUT for various thicknesses of the SiN_x layer are shown in Fig. 6. The resonance frequencies of the pMUT are a few MHz for any SiN_x thickness, which are the target frequency in medical applications. The 1st resonance frequency, f_r, of a simple clamped circular diaphragm is calculated by the following equation,[2]

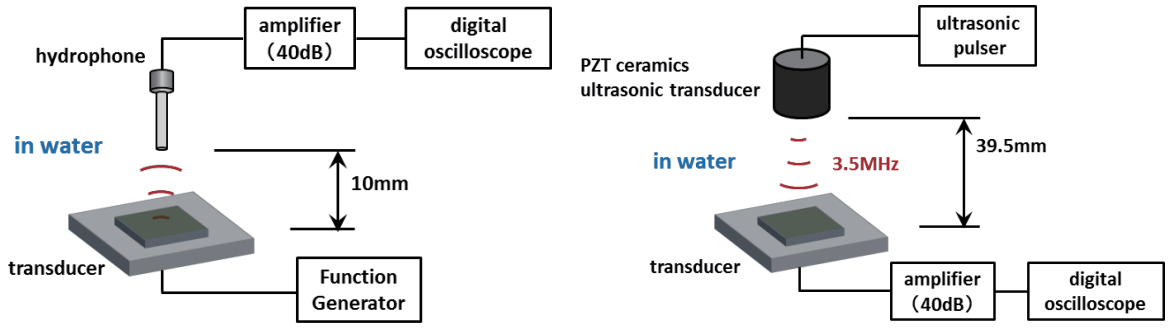

(a) (b)

Fig. 4. (Color online) Schematic of ultrasonic characterization system: (a) transmitting experiment and (b) receiving system.

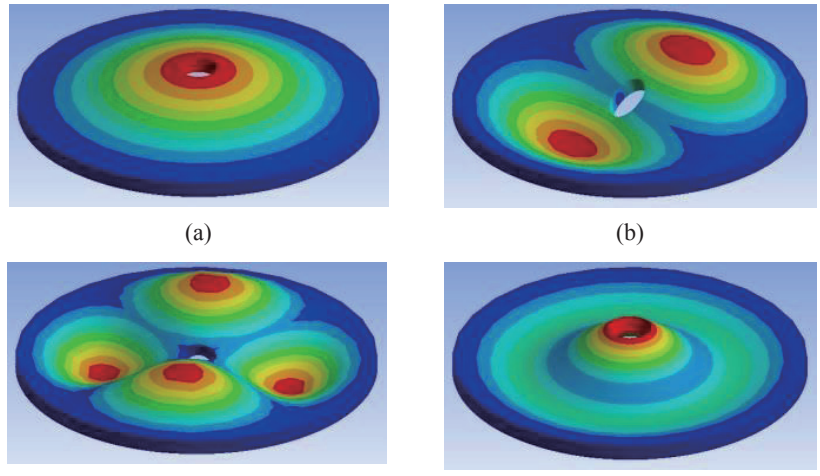

(a) (b)

(c) (d)

Fig. 5. (Color online) Resonant mode shapes and resonance frequency of pMUT from FEM analysis (SiN_x 0.5 μm): (a) 1st mode, 1.18 MHz; (b) 2nd mode, 2.47 MHz; (c) 3rd mode, 4.01 MHz; and (d) 4th mode, 4.59 MHz.

$$f_r = 0.5\frac{t}{a^2}\sqrt{\frac{E}{\rho}}, \tag{1}$$

where t is the diaphragm thickness, a is the diaphragm radius, E is the Young's modulus of the diaphragm, and ρ is the density of the diaphragm. According to eq. (1), the resonance frequency is proportional to the diaphragm thickness t, which concurs well with the FEM results. The vibration magnitude of the present pMUT becomes larger than that of the previous pMUT on decreasing the thickness of the SiN_x layer. The SiN_x layer should at least be 0.5 μm thick to achieve good insulation between the Al-Si wiring

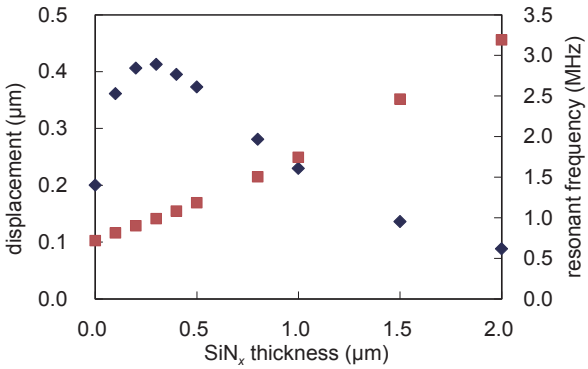

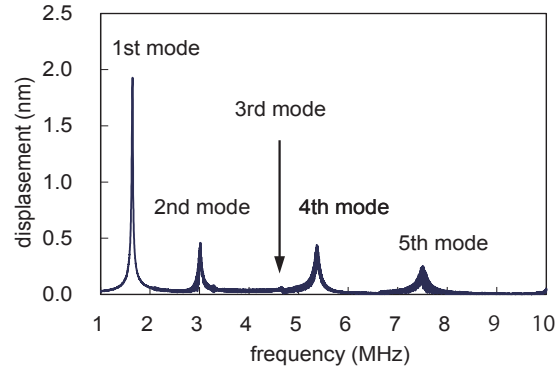

Fig. 6 (left). (Color online) FEM results of vibration magnitude and resonance frequency of pMUT for various SiN_x thicknesses.
Fig. 7 (right). (Color online) Frequency spectrum of center of pMUT measured by scanning LDV.

and the Pt bottom electrode, so the optimal SiN thickness was determined to be 0.5 μm. By changing the SiN_x thickness from 1.0 to 0.5 μm, the vibration magnitude becomes 1.7 times larger.

3.2 *LDV measurement*

Figure 7 shows the frequency spectrum at the center of the pMUT measured by the scanning LDV. The pMUT was excited by applying a 4 V_{pp} periodic sine wave on the electrodes. Five resonant modes appeared between 1 and 10 MHz, and the resonant mode shapes are shown in Fig. 8. Each shape is the same as in the FEM results. However, the resonance frequencies are higher than the results shown in Fig. 5. This suggests that the cavity of the fabricated pMUT is smaller than the designed size of 100 μm. According to eq. (1), the smaller the diaphragm radius a, the higher is the resonance frequency.

The vibration magnitude at the 1st mode resonance frequency of the fabricated pMUT and the previous pMUT measured by the LDV is shown in Fig. 9. This result reveals that the vibration magnitude of the fabricated pMUT became about threefold that of the previous pMUT by changing the thickness of the SiN_x from 1.0 to 0.5 μm. From the FEM analysis, a 1.7 times larger vibration magnitude was expected by changing the SiN_x thickness, however, the LDV measurement results show a significantly better value. In addition, the absolute values of the vibration magnitude differ significantly between the analysis results and experimental results: 373 nm in the FEM analysis and 1.64 nm in the LDV measurement. These differences occur because of differences in measurement conditions and material properties. In the FEM analysis, the vibration of the pMUT was a steady state response at the resonance frequency because the 1st resonance frequency was only contained in the applied voltage. On the other hand, the sweep frequency from 1 to 10 MHz was used as the applied voltage in LDV measurments; therefore, the vibration was not a steady state response. In addition, the surrounding atmosphere is

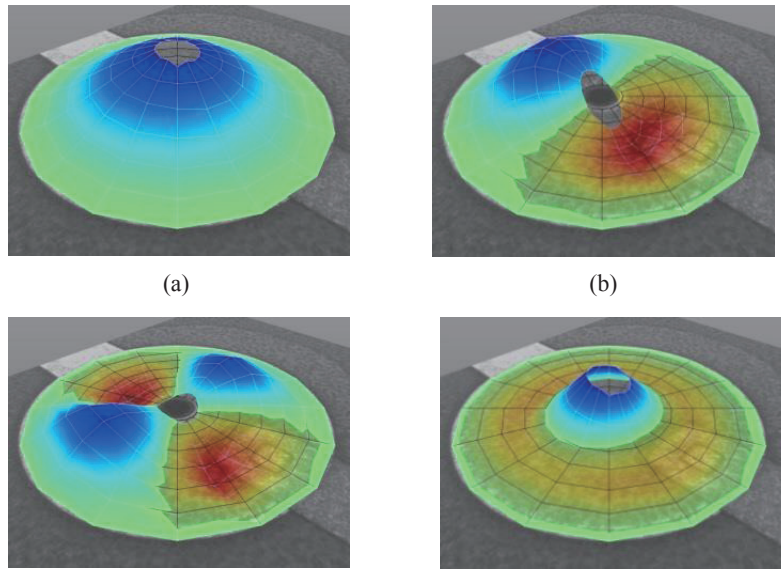

(a) (b)

(c) (d)

Fig. 8. (Color online) Resonance mode shapes and resonance frequencies of the pMUT measured by LDV: (a) 1st mode, 1.69 MHz; (b) 2nd mode, 3.20 MHz; (c) 3rd mode, 4.84 MHz; and (d) 4th mode, 5.66 MHz.

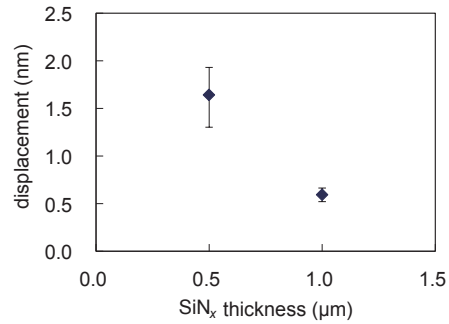

Fig. 9. (Color online) SiN_x thickness dependence of vibration magnitude.

different between the FEM analysis and the LDV measurements: a vacuum in the FEM analysis and air in the LDV measurements. Consequently, the vibration magnitude of the pMUT in the LDV measurements is smaller than that in the FEM analysis. In addition, differences in the materials used for the FEM analysis and the LDV measurements are also reasons for these differing results.

3.3 *Ultrasonic transmitting and receiving experiments*

A transmitted ultrasonic waveform generated by the fabricated pMUT was successfully observed by the hydrophone, which is shown in Fig. 10. The applied

voltage to the pMUT was a 10 V_{pp}, 2 MHz, 5 cycle sine burst wave. From the waveform and the ultrasonic sensitivity of the hydrophone, the sound pressure of the transmitted ultrasonic wave 1.0 cm from the pMUT was calculated and compared with the results of a previous study,[9] as shown in Fig. 11. From Fig. 11, it is seen that by changing the SiN_x thickness from 1.0 to 0.5 μm, the transmitted ultrasonic sound pressure increased approximately 11-fold.

Figure 12 shows received signal vs ultrasonic sound pressure characteristics of the fabricated pMUT and the previous pMUT. The ultrasonic sensitivities of the new and previous pMUTs were 19.8 and 3.83 μV/kPa, respectively. This result shows that the ultrasonic sensitivity of the new pMUT was about fivefold that of the previous pMUT. From these results, it is seen that the ultrasonic transmitting and receiving characteristics of the pMUT were improved by changing the structure according to the FEM analysis.

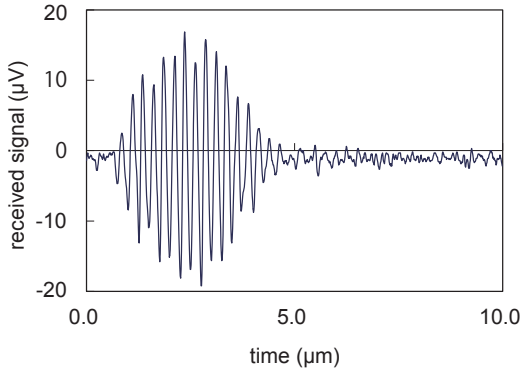

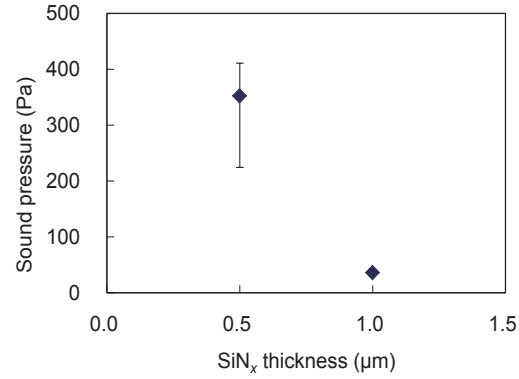

Fig. 10 (left). (Color online) Received ultrasonic waveform by hydrophone transmitted from pMUT.
Fig. 11 (right). (Color online) Ultrasonic sound pressure transmitted by new and previous pMUTs.

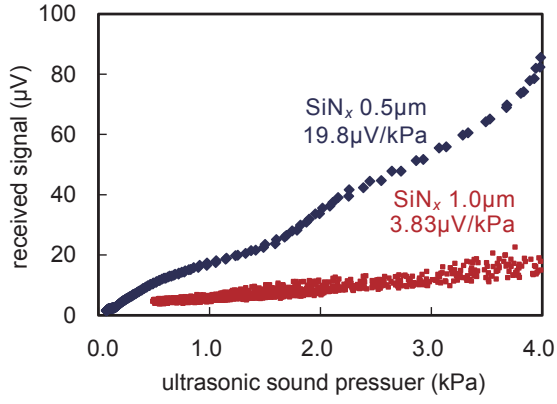

Fig. 12. (Color online) Received signal to ultrasonic sound pressure characteristics of fabricated pMUT and previous pMUT.

4. Conclusions

In this work, to improve the characteristics of the pMUT, the structure of the pMUT was investigated using FEM analysis. From the results of the FEM analysis using ANSYS, the vibration magnitude increased 1.7-fold by changing the SiN_x thickness from 1.0 to 0.5 μm. According to this result, a new pMUT with a 0.5-μm-thick SiN_x layer was fabricated and evaluated. The new pMUT shows a 3 times larger vibration magnitude, 11 times larger transmitted ultrasonic sound pressure, and 5 times larger ultrasonic sensitivity than those of the previous pMUT. This pMUT can be applied to miniature 2D pMUT arrays for 3D ultrasonic imaging.

Acknowledgements

The authors would like to thank Professor Yoshio Mita associated with the University of Tokyo for help in scanning LDV measurement in the Nanotechnology Platform Project sponsored by the Ministry of Education, Culture, Sports, Science and Technology (MEXT), Japan.

References

1 R. Swartz and J. Plummer: IEEE Trans. Electron Devices **26** (1979) 1921.
2 J. Bernstein, S. Finberg, K. Houston, L. Niles, H. Chen, L. Cross, K. Li and K. Udayakumar: IEEE Trans. Ultrason. Ferroelectr. Freq. Control **44** (1997) 960.
3 K. Yamashita, H. Katata, M. Okuyama, H. Miyoshi, G. Kato, S. Aoyagi and Y. Suzuki: Sens. Actuators, A **97**–**98** (2002) 302.
4 F. Akasheh, T. Myers, J. D. Fraser, S. Bose and A. Bandyopadhyay: Sens. Actuators, A **111** (2004) 275.
5 S. Machida, T. Kobayashi, M. Degawa, T. Takezaki, H. Tanaka, S. Migitaka, K. Hashiba, H. Enomoto, T. Nagata, Y. Yoshimura, K. Asafusa, K. Ishida, S. Sano and M. Izumi: Transducers 2009 Tech. Dig. (2009) 2218.
6 E. Cianci, A. Schina, A. Minotti, S. Quaresima and V. Foglietti: Sens. Actuators, A **127** (2006) 80.
7 D. Akai, Y. Ohba, N. Okada, M. Ito, K. Sawada, H. Takao and M. Ishida: Sens. Mater. **18** (2006) 161.
8 M. Ito, N. Okada, M. Takabe, M. Otonari, D. Akai, K. Sawada and M. Ishida: Sens. Actuators, A **145**–**146** (2008) 278.
9 D. Akai, K. Ozaki, Y. Numata, K. Suzuki, N. Okada and M. Ishida: Jpn. J. Appl. Phys. **51** (2012) 11PA04.
10 J. Rena, H. Zhanga, S. Liua and J. Wanga: Sens. Actuators, B **123** (2007) 135.
11 G. Vasta, T. Jackson, A. Frommhold, J. Bowen and E. Tarte: J. Electroceram. **27** (2011) 176.
12 A. Khan, J. Philip and P. Hess: J. Appl. Phys. **95** (2004) 1667.
13 Dupont: Dupont Kapton HN Polyimide Film Technical Data Sheet, http://www2.dupont.com/Kapton/en_US/assets/downloads/pdf/HN_datasheet.pdf (accessed in June 2014).
14 P. Muralt, N. Ledermann, J. Paborowski, A. Barzegar, S. Gentil, B. Belgacem, S. Petitgrand, A. Bosseboeuf and N. Setter: IEEE Trans. Ultrason. Ferroelectr. Freq. Control **52** (2005) 12.
15 H. Wado, T. Shimizu and M. Ishida: Appl. Phys. Lett. **67** (1995) 2200.
16 EASTEK HP: Acoustic Intensity Measurment System, http://www.eastek.co.jp/pages/supersonic_wave_pages/ultrasound.html (accessed in June 2014).